International Journal of the Physical Sciences Vol. 5(12), pp. 1857-1868, 4 October, 2010
Available online at http://www.academicjournals.org/IJPS
ISSN 1992 - 1950 ©2010 Academic Journals

Full Length Research Paper

Analytical solution of two-dimensional model of blood flow with variable viscosity through an indented artery due to LDL effect in the presence of magnetic field

Jagdish Singh[1] and Rajbala Rathee[2]*

[1]Department of Mathematics, Maharishi Dayanand University, Rohtak (Haryana), India.
[2]Department of Mathematics, Matu Ram Institute of Engineering and Management, Delhi Road, Rohtak-124001(Haryana), India.

Accepted 27 September, 2010

The present study is two-dimensional analysis of blood flow with variable viscosity through stenotic artery in the presence of transverse magnetic field in the porous medium. Blood flowing radially to walls of artery and axially through lumen has been determined through the solution of Navier Stoke's equations and Darcy law. If deposition of low density lipoprotein (LDL) is taken into case, the coupled approach offers an understanding of practical problem of blood flow through stenosed artery. The analytical expressions for radial velocity, axial velocity, shear stress and pressure gradient are obtained in the presence of magnetic field using Frobenius method. The numerical results for radial velocity, axial velocity, pressure gradient and shear stress are expressed graphically. The results then obtained are discussed to provide physical interpretation. The investigation shows that hypertensive patients are more adequate to have heart circulatory problems.

Key words: Indented artery, two-dimensional blood flow, shear stress, magnetic field, radial velocity, variable viscosity, Hematocrit.

INTRODUCTION

The abnormal growth, reducing the lumen of artery is called stenosis (atherosclerosis). This can cause serious problems by reducing the blood supply. One of the reasons for formation of stenosis is accumulation of macromolecules or low density lipoproteins on the arterial wall. The concept of transport of molecules to walls of artery has been supported by many researchers. Deposition of LDL along the walls of artery can greatly affect the velocity of blood flowing through artery, which ultimately affects the pressure of blood. The sudden changes in blood pressure of human body can collapse the heart of human being resulting in chances of sudden death.

Oka and Murata (1970) gave hydrodynamical theory of steady motion of blood through capillary with permeable wall. They were much interested to consider the exchange of fluid across the permeable wall. Many researchers have contributed in this field of research. Kenyon (1979) developed mathematical model of water flux through aortic tissue. Schneiderman et al. (1979) studied abnormalities in the exchange of substances between the arterial wall and the blood flowing within the lumen. Klancher and Tarbeill (1987) discussed a simple model of water flow through deformable porous media with emphasis on application to arterial walls. They

*Corresponding author. E-mail: anjalisidharath@gmail.com. Tel: +91-9729102043. Fax: 01262-272649.

modeled radially directed transport of water through arterial tissue, which is very important because transmural flow plays a significant role in accumulation of low density lipoproteins on the arterial walls.

In general, biological systems are affected by an application of external magnetic field on blood flow, through human arterial system. Haldar and Ghosh (1994) discussed the effect of magnetic field on blood flow through a stenosed artery. Sanyal and Maji (1999) discussed a mathematical model of unsteady blood flow in the presence of mild stenosis. The effect of pressure gradient and wall shear stress on flow was obtained and shown graphically. Dash and Mehta (1996) studied casson blood flow in homogeneous porous medium. This analysis exactly fits on pathological condition of artery, where fatty plaques of cholesterol are formed in the lumen of the coronary artery. They applied Brinkman model on the Newtonian flow through a porous media in a tube. Mazumdar et al. (1996) have discussed the pulsatile flow of blood through constricted artery and computed the results for axial velocity and pressure gradient and shown graphically. Sanyal and Maiti (1998) investigated the effect of externally applied magnetic field on the pulsatile flow of blood through a stenosed artery. Numerical solutions of axial velocity and pressure gradient have been discussed graphically.

Stangeby and Eithier (2002) worked out the coupled model of luminal blood flow and transmural fluid flow which was achieved through use of Brinkman's model, extension of Navier stokes equation in porous media. These equations are solved by using Petrov-Galerkin finite element method. Chakravarty and Sen (2005) have presented mathematical model describing the dynamic response of heat and mass transfer in blood flow through bifurcated arteries under stenotic condition. Ai and Vafai (2006) developed coupled model of transport of macro molecules in the blood flow and in the arterial walls. They used this model to simulate the LDL transport in a stenosed artery with various area reductions and stenosis numbers. Rathod and Tanveer (2009), discussed pulsatile flow of blood through porous medium under the influence of periodic body acceleration by considering blood as couple stress fluid. They studied effects of magnetic field, body acceleration and permeability parameter with the help of graphs. The effect of body acceleration on pulsalite flow of Casson fluid through mild stenosed artery has been investigated by Nagarani and Sarojamma (2008). They solved the involved non-linear equations using perturbation analysis. Sapna (2009) analyzed power law blood flow through constricted artery and explained results for resistance to flow, apparent viscosity and wall shear stress numerically.

In the present study, we discuss luminal blood flow along with the deposit of macromolecules to the walls of artery, which is being the main contributing factor for the development of stenosis in arteries here. The effect of externally applied transverse magnetic field over two-dimensional blood flow with homogenous porous medium and variable viscosity has been considered. The induced magnetic field has been neglected without loss of generality.

MATHEMATICAL MODEL

It is known that blood is complex fluid with erythrocytes, leucocytes, thrombocytes suspended in plasma. But, major part of plasma is occupied by erythrocytes. In the present model, the viscosity of blood depends on the concentration of cells in the whole blood, known as hematocrit. Therefore viscosity of blood is allowed to vary radially. The coefficient of viscosity of blood, given by Einstein, is

$$\mu^*(r^*) = \mu_0^* \left[1 + \beta h(r^*)\right] \tag{1}$$

where μ_0^* is the coefficient of viscosity of plasma and h(r*) is hematocrit described by the formula

$$h(r^*) = h_m \left[1 - \left(\frac{r^*}{R_0}\right)^n\right] \tag{2}$$

In equation (2), R_0 is the radius of normal tube, h_m is the maximum hematocrit at the centre of the tube and n is the parameter determining the shape of profile.

In this present problem, we consider n = 2, so that

$$\mu^*(r^*) = \mu_0^* \left\{1 + k\left(1 - \frac{r^{*2}}{R_0^2}\right)\right\}$$

or

$$\mu^*(r^*) = \mu_0^* \left\{a - k\frac{r^{*2}}{R_0^2}\right\} \tag{3}$$

where, $k = \beta h_m$, $a = 1 + k$.

The stenosis develops symmetrically about the axis and non-symmetric with respect to radial coordinates and its geometry has been described by Haldar and Ghosh (1994).

$$\frac{R^*(z^*)}{R_0} = 1 - A\left[l_0{}^{s-1}(z^* - d) - (z^* - d)^s\right], \; d \le z^* \le d + l_0 \tag{4}$$

where s($\geq$ 2) is a parameter determining the shape of stenosis, R*(z*) is radius of stenosed artery, l_0 is length of stenosis and d indicates its location.

In equation (4), A is given by

$$A = \frac{\in}{R_0 l_0^{\,s}} \frac{s^{s/s-1}}{s-1}$$

where $\in$ denoted the maximum height of stenosis at

$$z^* = d + \frac{l_0}{s^{1/s-1}}$$

such that $\in / R_0 << 1$.

We consider steady, laminar, incompressible and axially symmetric developed flow of blood with variable viscosity through an artery with mild stenosis under the influence of transverse magnetic field which is governed by the equations:

$$\rho^*\left(v_r^*\frac{\partial v_r^*}{\partial r^*}+v_z^*\frac{\partial v_r^*}{\partial z^*}\right)=-\frac{\partial P^*}{\partial r^*}+\frac{2\partial v_r^*}{\partial r^*}\frac{\partial \mu^*}{\partial r^*}$$
$$+\mu^*\left[\frac{\partial^2 v_r^*}{\partial r^{*2}}+\frac{1}{r^*}\frac{\partial v_r^*}{\partial r^*}+\frac{\partial^2 v_r^*}{\partial z^{*2}}-\frac{v_r^*}{r^{*2}}\right] \quad (5)$$
$$\rho^*\left(v_r^*\frac{\partial v_z^*}{\partial r^*}+v_z^*\frac{\partial v_z^*}{\partial z^*}\right)=-\frac{\partial P^*}{\partial z^*}+\frac{\partial \mu^*}{\partial r^*}\left(\frac{\partial v_r^*}{\partial z^*}+\frac{\partial v_z^*}{\partial r^*}\right)$$

$$+\mu^*\left[\frac{\partial^2 v_z^*}{\partial r^{*2}}+\frac{1}{r^*}\frac{\partial v_z^*}{\partial r^*}+\frac{\partial^2 v_z^*}{\partial z^{*2}}\right]-H^{*2}\sigma_e^* v_z^* \quad (6)$$

$$\frac{\partial v_r^*}{\partial r^*}+\frac{v_z^*}{r^*}+\frac{\partial v_z^*}{\partial z^*}=0. \quad (7)$$

The flow of fluid through porous walls is given by Darcy law

$$\frac{dP^*}{dr^*}=-\frac{\mu^*}{K^*}W^* \quad (8)$$

where W^* is filtration velocity, K^* is permeability constant and equation of continuity is given by

$$\frac{d}{dr^*}\left(r^*W^*\right)=0. \quad (9)$$

The corresponding boundary conditions are given as follows:

$$\text{At } r^*=0, \qquad v_r^*=0, \qquad \frac{\partial v_z^*}{\partial r^*}=0. \quad (10)$$

$$\text{At } r^*=R^*(z), \qquad v_z^*=0, \qquad v_r^*=W^*. \quad (11)$$

Fluid exchange across the wall is given by

$$v_r^* = K_f^*\left(P_0^*-P_{ext}^*\right) \quad (12)$$

where P_0^* and P_{ext}^* are prescribed pressures at inside and outside the wall of artery. Due to deposits of high cholesterol from the blood, ultimately forms the stenosis. It is to be specifically mentioned here that for the low density lipoproteins (LDL) transport to walls of artery, the radial velocity plays important role as they move in this direction. Let us consider $\in=\frac{R_0}{L}$, where L is the characteristic length of the artery and ε is perturbation parameter. We introduce non-dimensional scheme as follows:

$$r=\frac{r^*}{R_0},\ z=\frac{z^*}{L},\ P=\frac{P^*}{\rho^* U_0^{*2}/\mathrm{Re}\in},\ \mathrm{Re}=\frac{U_0^* R_0}{\nu^*},\ \nu^*=\frac{\mu^*}{\rho^*}$$

$$\left(\in v_r, v_z\right)=\left(\frac{v^*_r}{U_0^*},\frac{v_z}{U_0^*}\right), K_f=\frac{\mu_0^* K^*_f}{\in^2 R_0}, K=\frac{K^*}{R_0^2},\ \tau_{rz}=\frac{\tau_{rz}*}{\mu_0^* U_0^*/R_0} \quad (13)$$

where ρ^* is the density of the fluid, U_0^* is the characteristic velocity and Re is Reynolds number. Using above non-dimensional scheme, the equations (3) and (5-9) in terms of non-dimensional variables, become

$$\mu(r)=\mu_0\left(a-kr^2\right)=\mu_0\Theta \quad (14)$$

$$\in\left[v_r\frac{\partial v_r}{\partial r}+v_z\frac{\partial v_r}{\partial z}\right]=\frac{1}{\mathrm{Re}}\left[-\frac{\partial P}{\partial r}+\frac{2\partial v_r}{\partial r}\frac{d\Theta}{dr}+\frac{\partial^2 v_r}{\partial r^2}\right.$$
$$\left.+\frac{1}{r}\frac{\partial v_r}{\partial r}+\frac{\in^2\partial^2 v_r}{\partial r^2}-\frac{v_r}{r^2}\right] \quad (15)$$

$$\in\left[v_r\frac{\partial v_z}{\partial r}+v_z\frac{\partial v_z}{\partial z}\right]=\frac{1}{\mathrm{Re}}\left[-\frac{\partial P}{\partial z}+\frac{d\Theta}{dr}\left\{\in^2\frac{\partial v_r}{\partial z}+\frac{\partial v_z}{\partial r}\right\}\right.$$
$$\left.+\Theta\left\{\frac{\partial^2 v_z}{\partial r^2}+\frac{1}{r}\frac{\partial v_z}{\partial r}+\frac{\in^2\partial^2 v_r}{\partial z^2}\right\}-M^2 v_z\right] \quad (16)$$

$$\frac{\partial v_r}{\partial r}+\frac{v_r}{r}+\frac{\partial v_z}{\partial z}=0 \quad (17)$$

$$\frac{dP}{dr}=\frac{\Theta}{K}W \quad (18)$$

$$\frac{d}{dr}(rW)=0 \quad (19)$$

where,

$$M=HR_0\left(\frac{\sigma_e}{\mu_0}\right)^{\frac{1}{2}}, \qquad \Theta=a-kr^2.$$

The boundary conditions in terms of non-dimensional variables are as follows:

At $r = 0,$ $v_r = 0$, $\frac{\partial v_z}{\partial r} = 0$. (20)

At $r = R(z),$ $v_z = 0$, $v_r = W$. (21)

The non-dimensional flux across any cross-section is prescribed by

$$\int_0^{R(z)} v_z r dr = \pi \tag{22}$$

Fluid exchange across the wall is given by

$$v_r = K \in^2 \left(P_0 - P_{ext}\right). \tag{23}$$

Using Perturbation technique, we can assume a solution in the form

$$\left(v_r,\ v_z,\ P\right) = \sum_0^{\infty} \in^j \left(v_{rj},\ v_{zj},\ P_j\right) \tag{24}$$

Substituting (24) in equations (15) – (17), we obtain

$$\frac{\partial^2 v_{r0}}{\partial r^2} + \frac{1}{r}\frac{\partial v_{r0}}{\partial r} + \frac{2\Theta}{\partial r} v_{r0} - \frac{v_{r0}}{r^2} = \frac{\partial P_0}{\partial r}$$

$$\frac{\partial^2 v_{z0}}{\partial r^2} + \frac{1}{r}\frac{\partial v_{z0}}{\partial r} + \frac{2\Theta}{\partial r}\frac{\partial v_{z0}}{\partial r} - M^2 v_{z0} = \frac{\partial P_0}{\partial z}$$

$$\frac{\partial v_{r0}}{\partial r} + \frac{v_{r0}}{r} + \frac{\partial v_{z0}}{\partial z} = 0 \tag{25}$$

etc.

We attempt here to determine the zeroth order solution for the axial velocity, radial velocity and pressure gradient. On integration of equation (19), we get

$$W = \frac{A_1}{r} \tag{26}$$

Equations (25) can be solved with the help of equations (18) and (26) using Frobenius method. It is required that v_{z0} is bounded at r = 0, the only possible series solutions of equations (25) are given by

$$v_{r0} = A\sum_{m=0}^{\infty} B_m r^{m-1} - \frac{A_1 k}{8aK}\sum_{m=0}^{\infty} \bar{B}_m r^{m+3} \tag{27}$$

where,

$$B_m = \frac{k\left[(m-3)(m+1)-1\right]}{am(m-2)} B_{m-2}, \quad m>2 \tag{28}$$

$$B_2 = -2B_0 \tag{29}$$

$$\bar{B}_m = \frac{k\left[(m+1)(m+5)-1\right]}{a(m+2)(m+4)} \bar{B}_{m-2}. \tag{30}$$

B_0 and $\bar{B}_0$ are taken as unity and $B_{m+1} = \bar{B}_{m+1} = 0$ (31)

and

$$v_{z0} = A_0\sum_{m=0}^{\infty} C_m r^m + \frac{1}{4a}\frac{dP_0}{dz}\sum_{m=0}^{\infty} \bar{C}_m r^{m+2} \tag{32}$$

such that

$$C_m = \frac{km(m-2) + M^2}{am^2} C_{m-2} \tag{33}$$

$$\bar{C}_m = \frac{km(m+2) + M^2}{a(m+2)^2} \bar{C}_{m-2}. \tag{34}$$

C_0 and $\bar{C}_0$ are taken as unity and $C_{m+1} = \bar{C}_{m+1} = 0$

On applying boundary conditions (21-23) on equations (27) and (31), we obtain

$$A_1 = R(z) K_f \in^2 \left(P_0 - P_{ext}\right) \tag{35}$$

$$A = \frac{K_f \in^2 \left(P_0 - P_{ext}\right)\left\{1 + \frac{k}{8aK}\sum_{m=0}^{\infty} \bar{B}_m \left[R(z)^{m+4}\right]\right\}}{\sum_{m=0}^{\infty} B_m \left[R(z)^m\right]} \tag{36}$$

$$A_0 = \frac{\pi\sum_{m=0}^{\infty} \bar{C}_m R(z)^{m+2}}{\sum_{m=0}^{\infty} \bar{C}_m R(z)^{m+2}\sum_{m=0}^{\infty}\frac{C_m R(z)^{m+2}}{m+2} - \sum_{m=0}^{\infty} C_m R(z)^m \sum_{m=0}^{\infty}\frac{\bar{C}_m R(z)^{m+4}}{m+4}} \tag{37}$$

$$\frac{dp}{dz} = \frac{-4a\pi\sum_{m=0}^{\infty} C_m R(z)^m}{\sum_{m=0}^{\infty} \bar{C}_m R(z)^{m+2}\sum_{m=0}^{\infty}\frac{C_m R(z)^{m+2}}{m+2} - \sum_{m=0}^{\infty} C_m R(z)^m \sum_{m=0}^{\infty}\frac{\bar{C}_m R(z)^{m+4}}{m+4}} \tag{38}$$

The non-dimensional shear stress on walls of artery is given by

$$\tau_{rz} = \left(a - kr^2\right)\left(\in^2 \frac{\partial v_r}{\partial z} + \frac{\partial v_z}{\partial r}\right)\Big|_{r=R(z)} \tag{39}$$

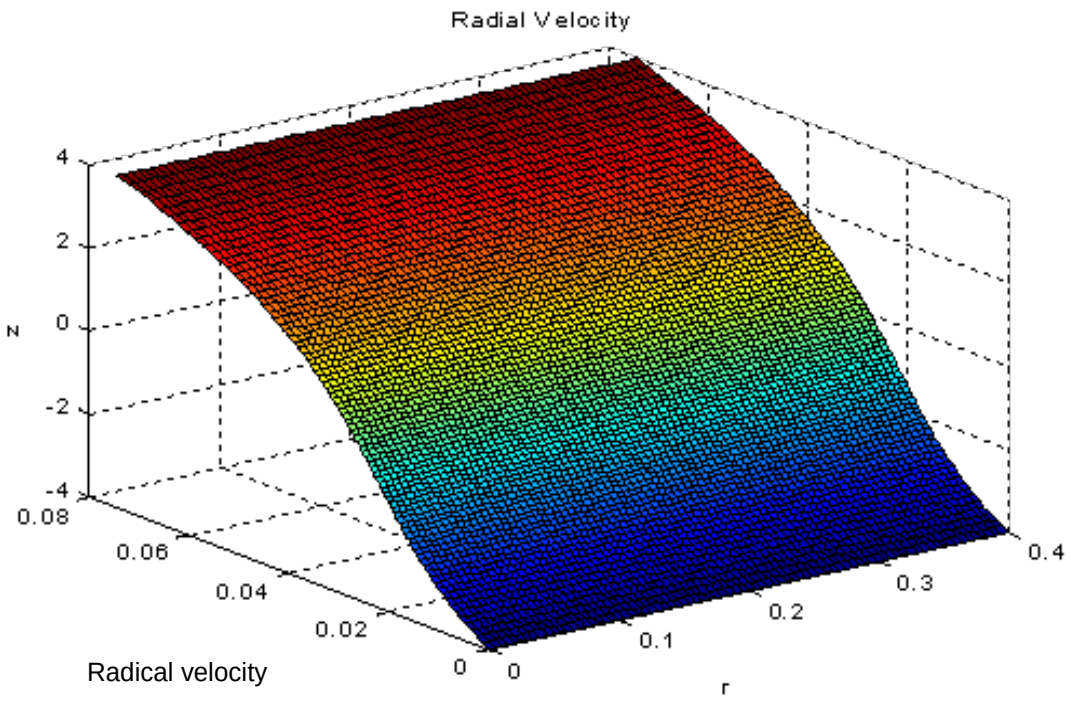

Figure 1. Two-dimensional variation of radial velocity at different radial and axial positions.

$$\frac{\left[a-kR^2(z)\right]K_f \in^2 R'(z)(P_0-P_{ext})\sum_{m=0}^{\infty}B_m(R(z))^{m-1}}{\left(\sum_{m=0}^{\infty}B_m\left(R(z)\right)^m\right)^2}\left[\frac{k}{8aK}\left\{\sum_{m=0}^{\infty}B_m\left(R(z)\right)^m\sum_{m=0}^{\infty}(m+4)\overline{B_m}\left(R(z)\right)^{m+3}-\right.\right.$$

$$\left.\left.\sum_{m=0}^{\infty}\overline{B_m}\left(R(z)\right)^{m+4}\sum_{m=0}^{\infty}mB_m\left(R(z)\right)^{m-1}-\sum_{m=0}^{\infty}\overline{B_m}\left(R(z)\right)^{m+3}\left(\sum_{m=0}^{\infty}B_m\left(R(z)\right)^m\right)^2\right\}-\sum_{m=0}^{\infty}mB_m\left(R(z)\right)^{m-1}\right] \quad (40)$$

$$\left[a-kR^2(z)\right]\left[A_0\sum_{m=0}^{\infty}mC_m\left(R(z)\right)^{m-1}+\frac{1}{4a}\frac{dP_0}{dz}\sum_{m=0}^{\infty}(m+2)\overline{C_m}\left(R(z)\right)^{m+1}\right]$$

RESULTS AND DISCUSSION

The shape of constriction considered for numerical computations is the same as in Haldar and Ghosh (1994). It is difficult to handle the problem with the extended notions considered herein, but computation with MATLAB 7.01 makes it easier to describe the numerical results graphically for the present investigation.

The flow investigation has been carried out by studying the effect of individual factors like magnetic field M, filtration coefficient K_f, permeability constant K, and parameter k which depends upon hematocrit. The main objective of the study is to find the role of magnetic field, parameter k, filtration coefficient, permeability constant on axial and radial velocity profiles, and pressure gradient at various axial and radial positions. Figure 1 shows the radial velocity profiles at different radial and axial positions. Here the radial velocity decreases with increase in z which is confirmed in Figure 2. Figure 2 shows radial velocity profiles at various transmural pressures, that is, $P=P_0-P_{ext}$. We observe from Figure 2 that, for an increase in transmural pressure, there is increase in radial velocity which results in increase of transmural filtration and ultimately changes the concentration at the maximum height of constriction. Therefore, the net uptake of LDL on arterial wall increases.

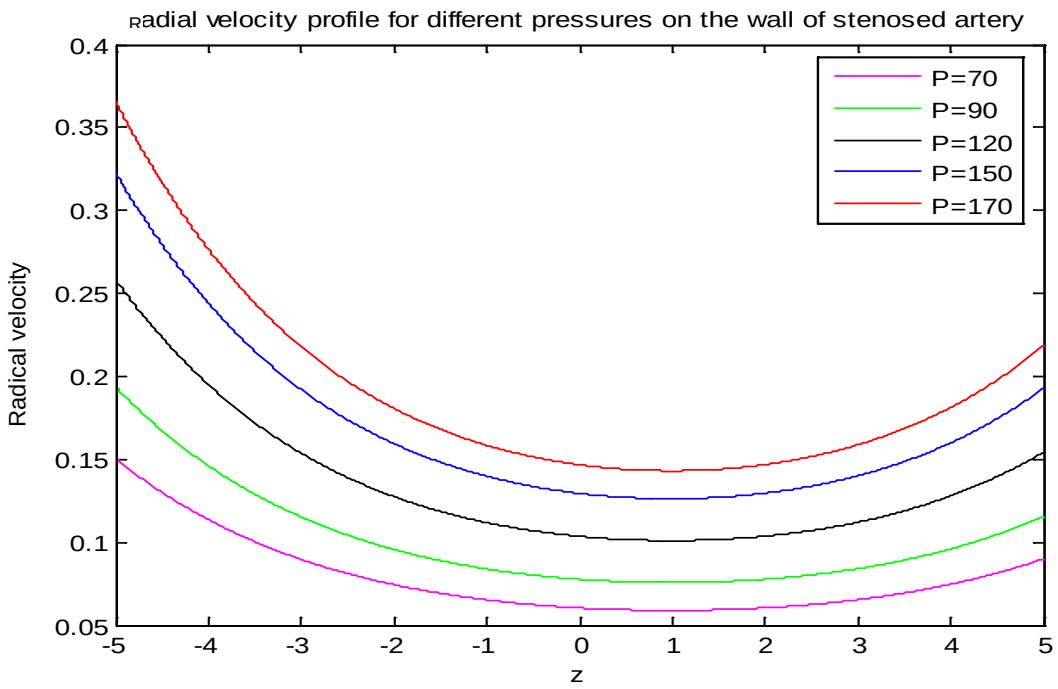

Figure 2. Variation of radial velocity with axis for different values of P.

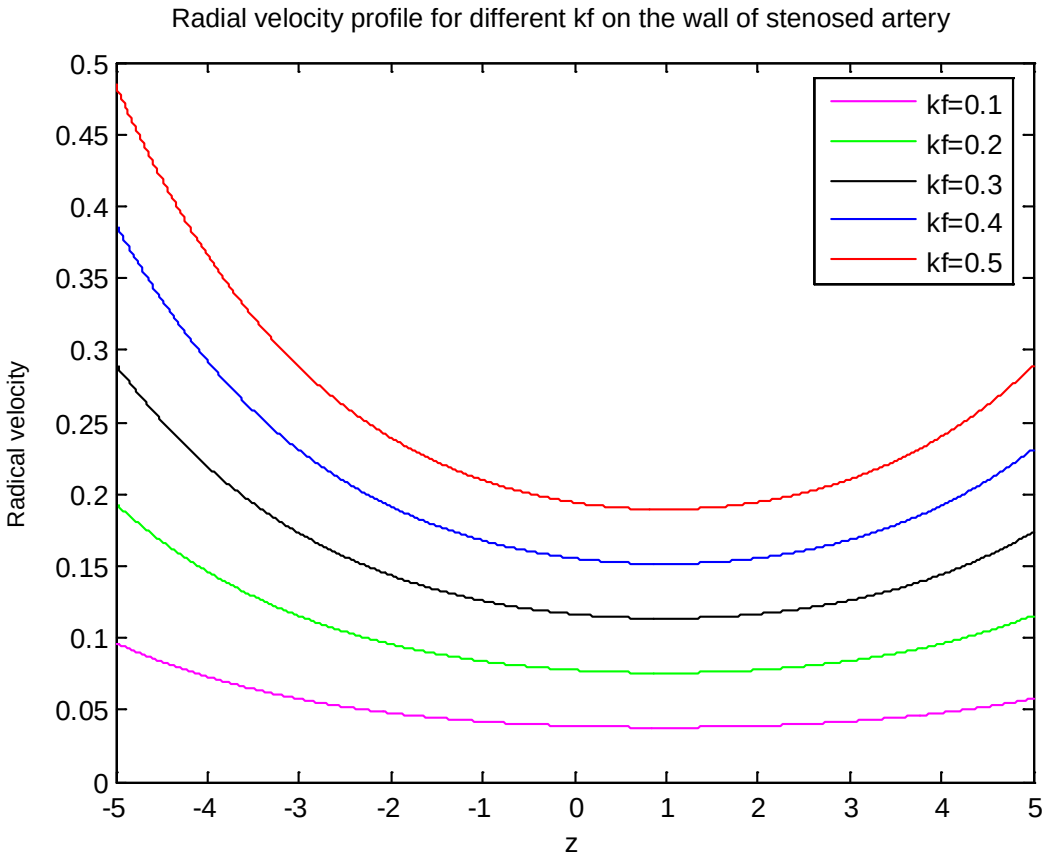

Figure 3. Variation of radial velocity with axis for different values of K_f .

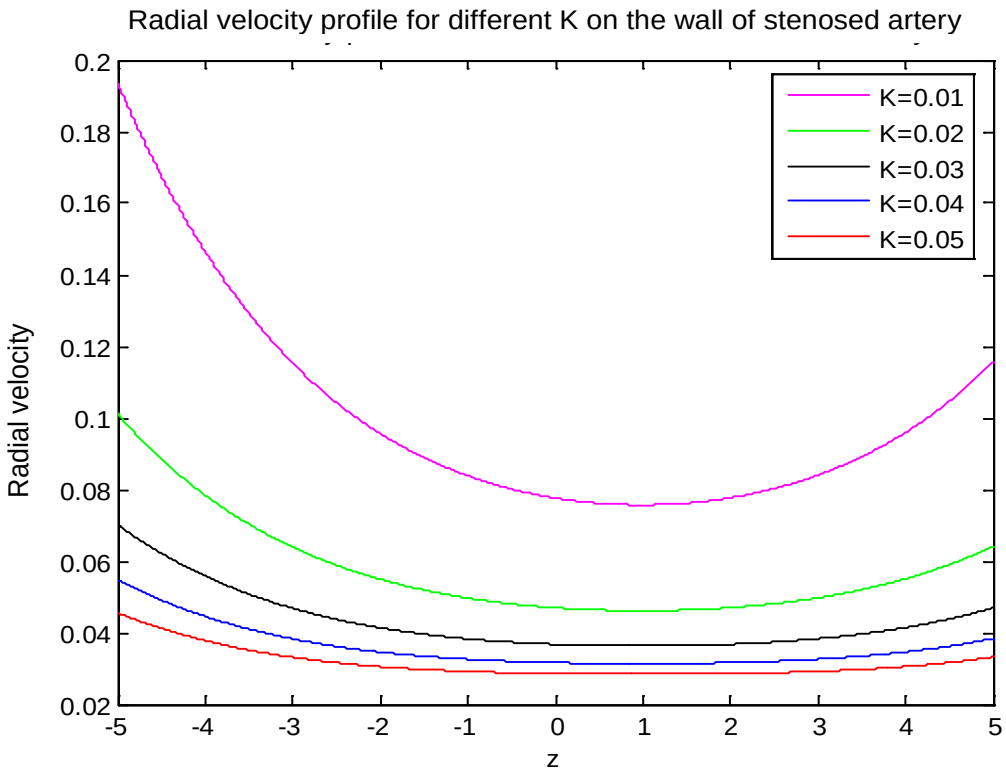

Figure 4. Variation of radial velocity along axis for different values of K.

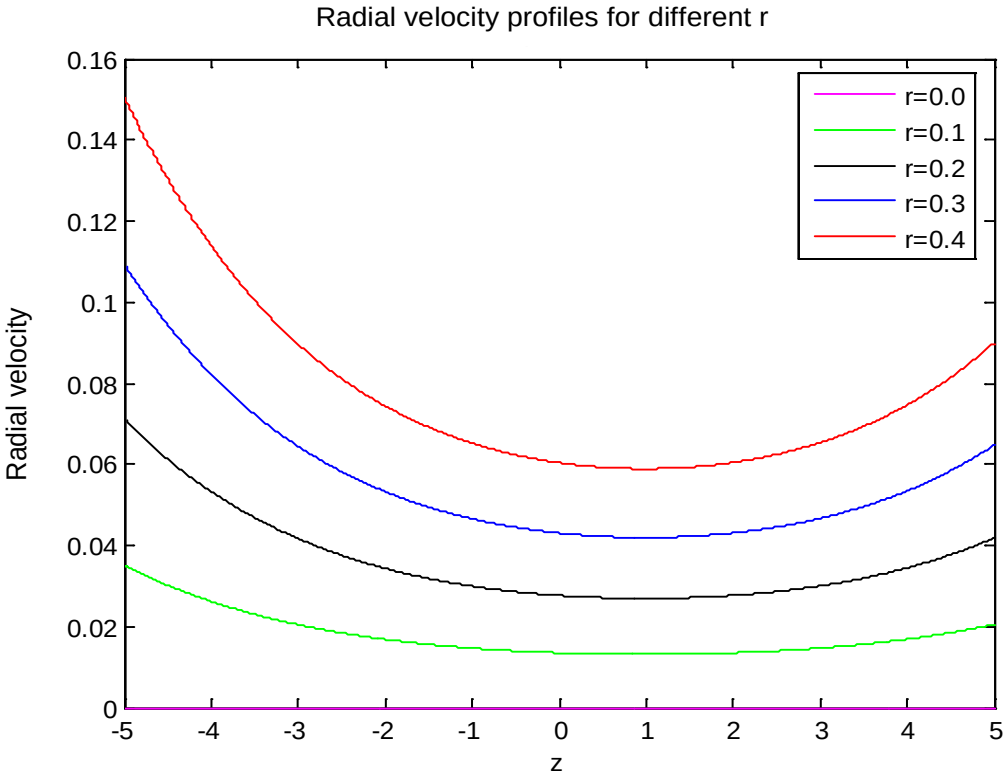

Figure 5. Variation of radial velocity with axis at different radial positions.

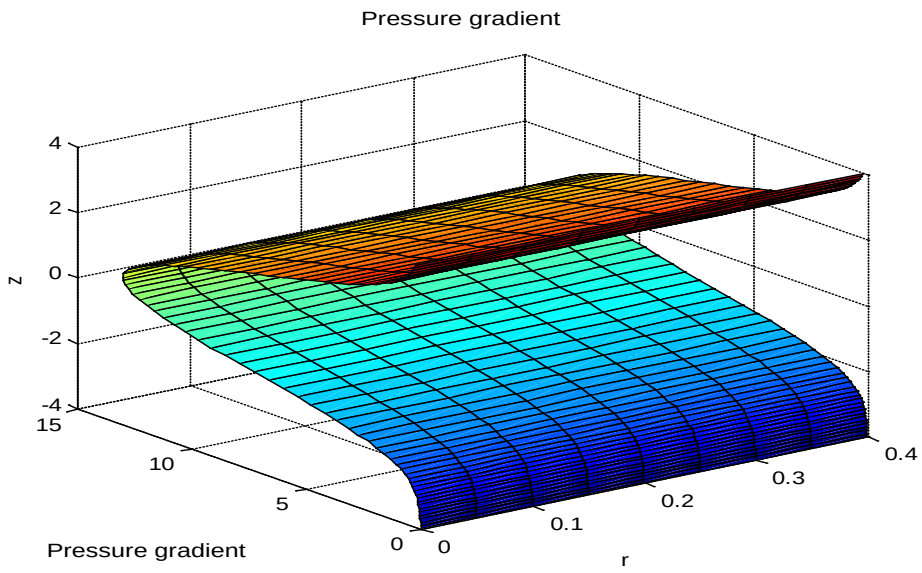

Figure 6. Two-dimensional variation of pressure gradient at different radial and axial positions.

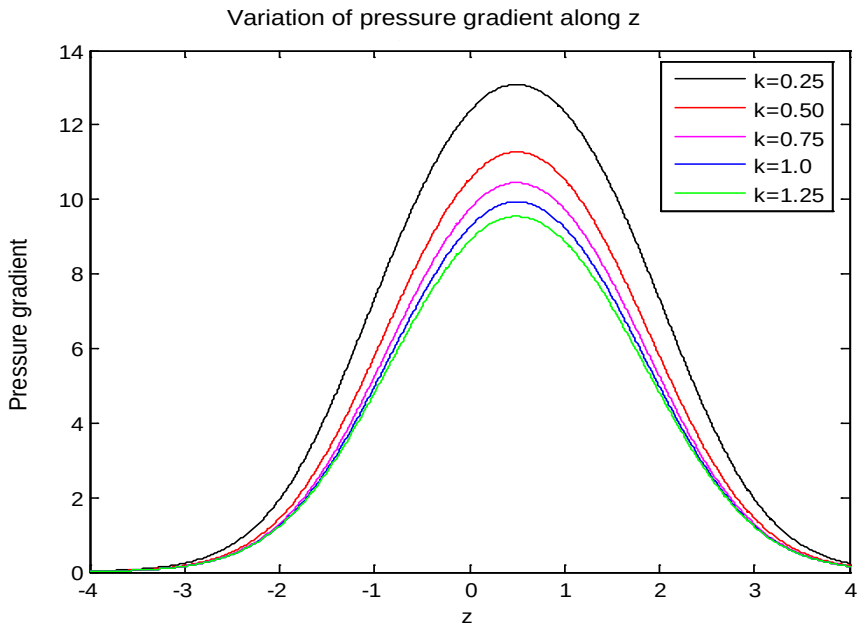

Figure 7. Variation of pressure gradient with axis for different values of k.

These numerical results are in agreement with the results obtained by Oka and Murata (1970). This is the reason that hypertensive patients are more prone to atherosclerosis. Figure 3 describes radial velocity at different values of filtration coefficient. We observe that filtration coefficient 'Kf' plays the same role as the transmural pressure because filtering deletes the obstacles of the flow significantly. The effect of filtration coefficient is much more pronounced as compared to increase in transmural pressure. Figure 4 shows radial velocity profiles for different values of permeability constant K. It is observed that radial velocity decreases as we move along stenosis and it is minimum at the peak of stenosis. Figure 5 represents the variation of radial velocity for different values of r. It shows that as we move away from the axis, the radial velocity increases, and on the axis, it is zero.

Figure 6 represents the variation of pressure gradient at both radial and axial positions simultaneously. It exhibits that as we move along the axis of the tube, the pressure gradient increases and it is maximum at the maximum height of stenosis and then decreases rapidly.

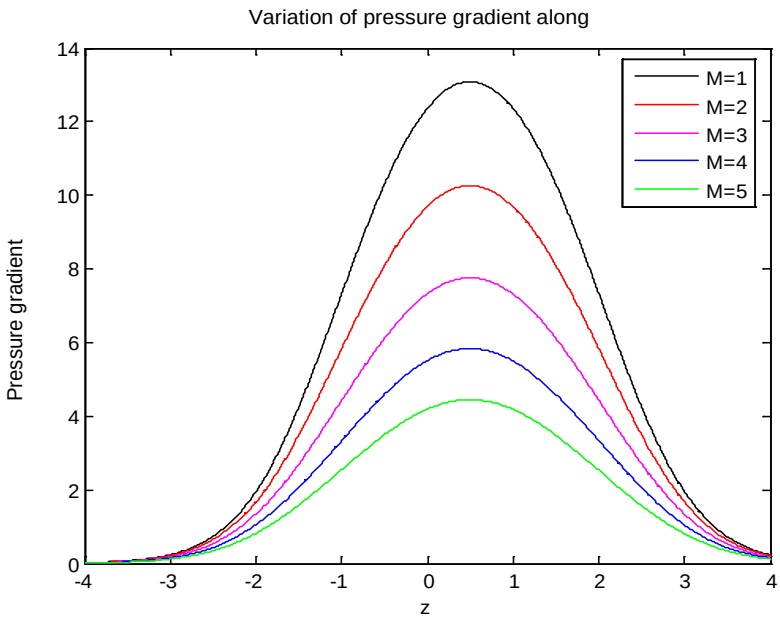

Figure 8. Variation of pressure gradient with axis for different values of M.

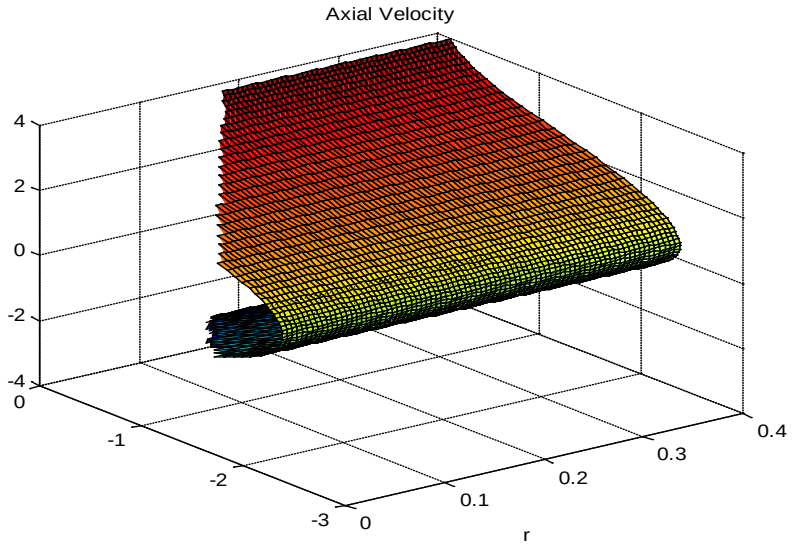

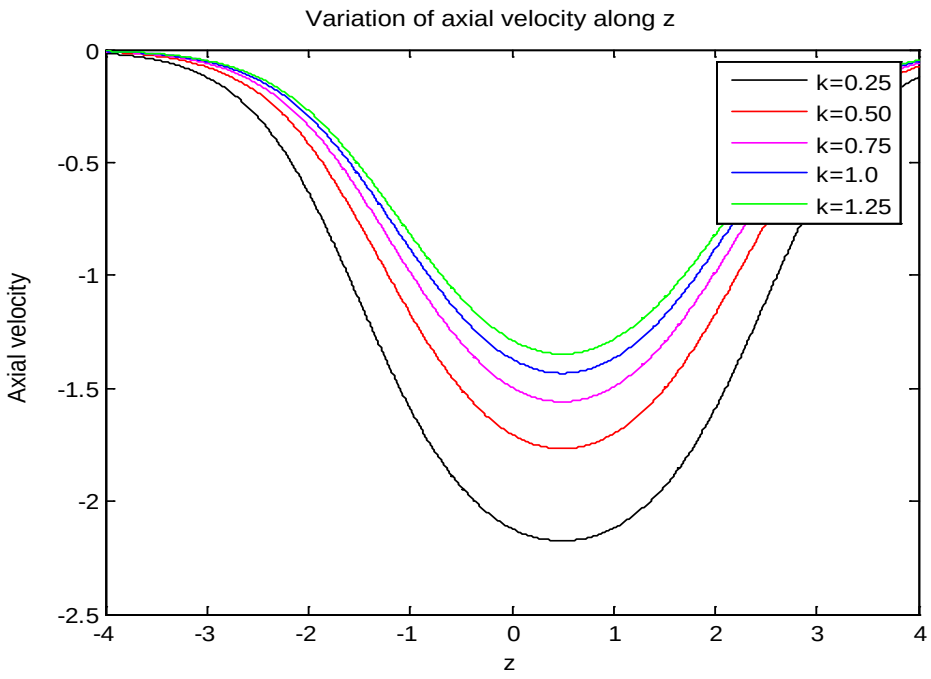

Figure 10. Variation of axial velocity with axis for different values of k.

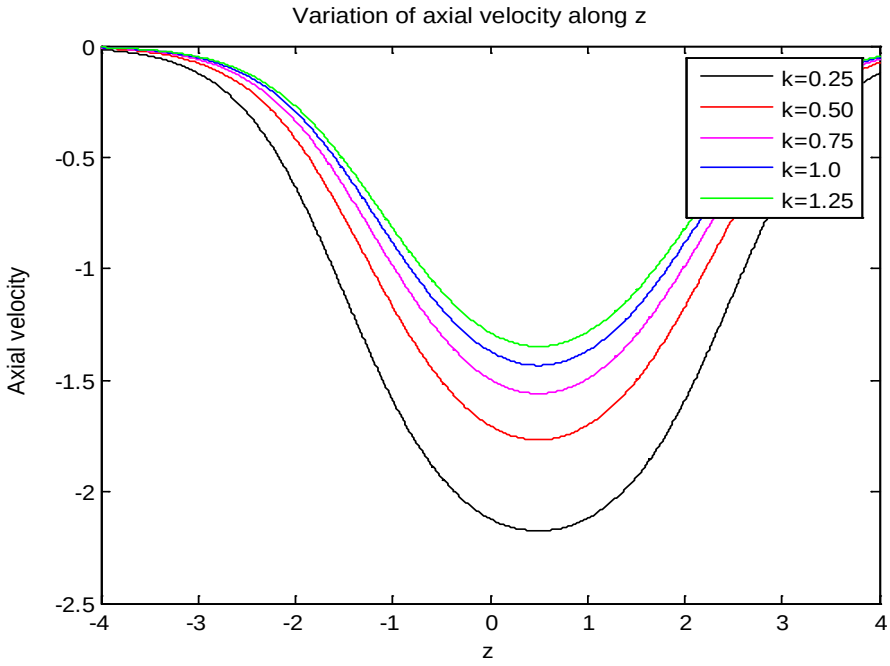

Figure 11. Variation of axial velocity with axis for different values of M.

the stenosis and then it again increases. It shows the signs of improper blood flow along the tube. As per Figure 10, the axial velocity increase with increase in the value of k. Similarly, Figure 11 demonstrates that increase in M(Hartmann number) increases the velocity which is physically also true. Figure 12 gives the com-- puted results for shear stress. It also shows the expected patterns and the results are comparable with various

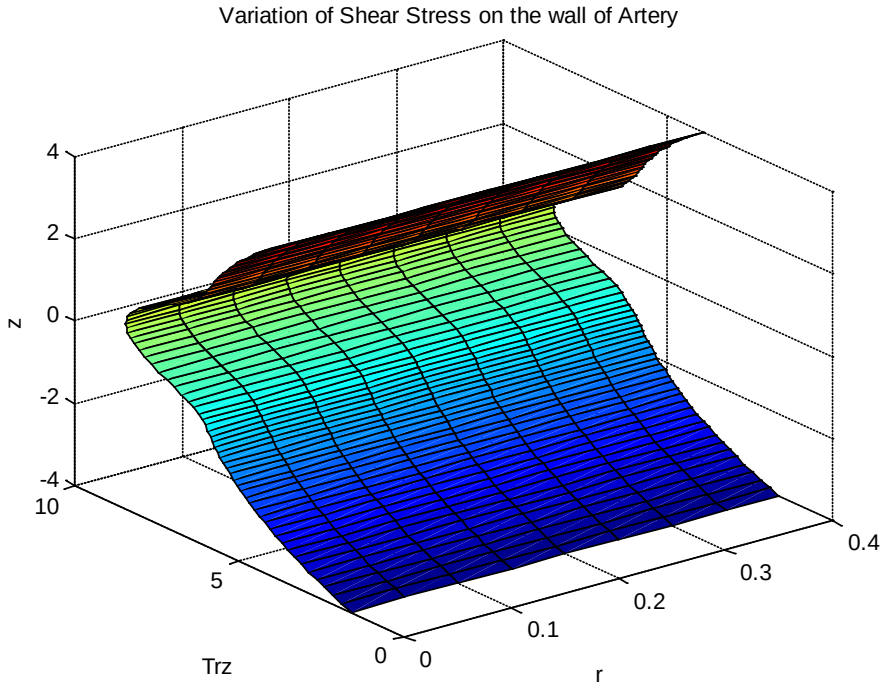

Figure 12. Two-dimensional variation of shear stress at different radial and axial positions.

previous studies. The shear stress is maximum at the peak of stenosis and then decreases.

Conclusions

Increase in radial velocity with increase in transmural pressure leads to more and more deposition of LDL at the maximum height of stenosis which shows that at the peak of stenosis, there would be maximum deposition in comparison to other positions of stenosis which results in intimal thickening of artery and makes it more stiffened in particular region causing disturbed flow patterns of blood.

The effect of increase in pressure gradient results in the rise in systolic pressure and fall in diastolic pressure, which are very harsh conditions for diseased heart.

The effect of magnetic field is more pronounced in comparison to hematocrit. Application of low strength magnetic field on stenosed artery can improve the blood flow up to some extent but application of high strength can cause death also.

Shear stress increases on the walls of artery as we move along the axis of tube but it is interesting to note that as we move close to the height of stenosis, it gives a sharp increase which is a remarkable effect on the walls of artery, causing disturbance in blood flow.

Walls shear stress increases as we move along the stenosis and then it decreases. It indicates that influence of shear stress on walls of artery leads to more and more deposition of LDL along the wall of artery.

It is evident from axial velocity that due to stenosis there is a back flow and hence velocity becomes negative at the stenosis.

REFERENCES

Ai L, Vafai K (2006). A coupling model for macromolecule transport in a stenosed arterial wall. Int. J. Heat Mass Transfer, 49: 1568-1591.

Chakravarty S, Sen S (2005). Dynamic response of heat and mass transfer in blood flow through stenosed bifurcated arteries. Korea-Australia Rheol. J., 17: 47-62.

Dash RK, Mehta KN (1996). Casson fluid flow in a pipe filled with a homogenous porous medium. Int. J. Eng., 54: 1145-1152.

Kenyon DK (1979). A mathematical model of water flux through Aortic tissue. Bull. Math. Biol., 41: 79.

Haldar K, Ghosh SN (1994). Effect of magnetic field on blood flow through an indented tube in the presence of erythrocytes. Indian J. Pure Appl. Math., 25: 345-352

Klancher M, Tarbeill JM (1987). Modelling water flow through arterial tissue, Bull. Mathematical Biol., 49: 651-669.

Mazumdar HP, Gangully UN, Gharai S, Dalal DC (1996). On the distributions of axial velocity and pressure gradient in a pulsatile flow of blood through constructed artery. Indian J. Pure Appl. Math., 27: 1137-1150.

Nagarani P, Sarojamma G (2008). Effect of body acceleration on pulsatile flow of Casson fluid through a mild stenosed artery. Korea-Australia Rheol. J., 20: 189-196.

Oka S, Murata T (1970). A theoretical study of the flow of blood in a capillary with permeable wall, Jpn. J. Appl. Phy., 9: 345-352.

Rathod VP, Tanveer S (2009). Pulsatile flow of couple stress fluid through a porous medium with periodic body acceleration and magnetic field. Bull. Malaysian Math. Sci. Soc., 32: 245-259.

Sanyal DC, Maiti AK (1998). On pulsatile flow of blood through a stenosed artery. Indian J. Math., 40: 199-213.

Sanyal DC, Maji NK (1999). Unsteady blood flow through an indented

tube with Atherosclerosis. Indian J. Pure Appl. Math., 30: 951-959.
Sapna S (2009). Analysis of non–newtonion fluid flow in a stenosed artery. Int. J. Phys. Sci., 4: 663-671.
Schneiderman G, Ellis GC, Goldstick TK (1979). Mass transport to walls of stenosed arteries: Variation with Reynolds number and blood flow separation. J. Biomech., 12: 869-877.
Stangeby DK, Eithier CR (2002). Computational analysis of coupled blood-wall arterial LDL transport, J. Biomech. Eng., 124: 1-8.